Overview of modelling the microstructural state of steel strip during hot rolling*

by I.V. Samarasekera† and E.B. Hawbolt†

Synopsis

A review of recent work being conducted at the University of British Columbia on the modelling of the microstructural evolution during the hot rolling of steel is presented.

A mathematical model of heat transfer was developed to describe the thermal field in a slab during rough and finish rolling. The model for rough rolling, discussed in this review, also simulates the growth of oxide scale on the slab surface. To quantify the heat transferred from the slab to the work rolls, instrumented samples of AISI 304 L stainless steel, 0,05 per cent carbon steel, and 0,05 per cent carbon steel with 0,025 per cent

Introduction

The future competitiveness of the steel industry will depend critically on its ability to tailor its products to meet stringent specifications with respect to quality and mechanical properties. In the area of steel-strip production, this has led to a worldwide effort directed towards the prediction of microstructural evolution with the aid of mathematical and physical models[1-17]. However, the research is in an evolutionary stage, moving away from being highly empirical to knowledge-intensive, with strong roots in transport phenomena, continuum mechanics, and physical metallurgy. Knowledge-based models provide a more scientific framework within which to effect process control and produce material with the desired shape, dimensions, and mechanical properties.

This paper describes recent work at the University of British Columbia (UBC), where strong emphasis has been placed not only on the description of microstructural changes but also on the accurate quantification of the thermo-mechanical history during rolling.

Modelling of the thermal field during rolling

Because of the profound influence of temperature on the flow stress of steel and on the structure-modifying processes such as static and dynamic recrystallization, grain growth, phase transformation, and precipitation, the basis of any attempt to predict the microstructural state of steel during rolling must begin with the characterization of the thermal field. Unfortunately, this is an area that has been neglected by researchers worldwide, and very little has been done to accurately quantify the thermal field, particularly in the roll-bite. Davadas *et al.*[12] were the first to show that the interface heat-transfer coefficient between the work roll and the strip is strongly influenced by rolling conditions such as rolling speed, reduction, and lubrication, and pointed to a link with pressure at the roll–steel interface. However, this initial work was conducted on stainless steel, and the direct applicability of the findings to other grades of steel was uncertain.

Recently, Chen *et al.*[18] rolled samples of 0,05 per cent carbon steel, 0,05 per cent carbon with 0,025 per cent niobium steel, and AISI 304L stainless steel at different temperatures, speeds, and reductions on the laboratory mill at UBC, and also on the pilot rolling mill at CANMET. To prevent excessive scale formation, the samples of carbon steel were heated in a tube furnace in an inert gas (N_2) atmosphere. The thermal response of the samples was monitored according to the procedure developed by Devadas *et al.*[12], and the heat-transfer coefficients at the roll–steel interfaces were calculated by a similar method.

Figure 1 compares the heat-transfer coefficients for three different steels under the conditions given in Table I. In all cases, the heat-transfer coefficient increased with increasing time as the sample progressed through the roll bite, reached a maximum, and subsequently decreased. This trend was also observed by Devadas *et al.*[12]. Furthermore, it is evident that the heat-transfer coefficient was highest for the micro-alloyed steel despite the lower reduction. Important, however, is the lower rolling temperature and the higher strength of the micro-alloyed steel, which gave rise to a higher pressure in the roll bite.

It has been postulated that, during rolling, higher pressure increases the contact area between the roll and the strip, enhancing heat transfer[12,19]. Further confirmation of this finding is seen in the results of Chen *et al.*[18] (Figure 2), in which there is a strong correlation between the mean heat-transfer coefficient and the mean pressure irrespective of material type or rolling conditions. It is therefore now possible to determine a mean heat-transfer coefficient for a given rolling pass from an estimate of the rolling loads and the mean pressure. This correlation between heat-transfer coefficient and pressure also allows the extrapolation of pilot- and laboratory-mill measurements to industrial operations with a greater degree of confidence.

---

* *Presented at the G.T. Van Rooyen Symposium 'Materials in Action', which was held at the University of Pretoria on 29th and 30th June, 1994.*

† *The Centre for Metallurgical Process Engineering, The Department of Metals and Materials Engineering, The University of British Columbia, Vancouver, B.C., Canada V6T 1Z4.*

ISSN 0038-223X/3.00 + 0.00.

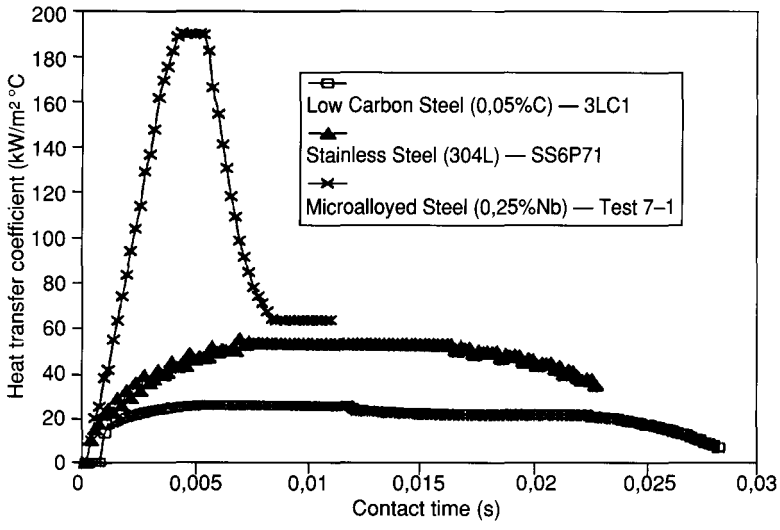

Figure 1—Heat-transfer coefficient at the roll–steel interface for three different materials

Table I

Conditions for instrumented rolling tests

Type of of material	Temp. °C	Initial thickness mm	Reduction %	Rolling speed m/s	Mean pressure kg/mm²
0,05 %C	1250	51,8	6,8	1,0	5,4
304L	1250	25,4	9,0	1,0	10,46
0,05 % C 0,025 % Nb	1050	11,8	2,6	0,3	20,14

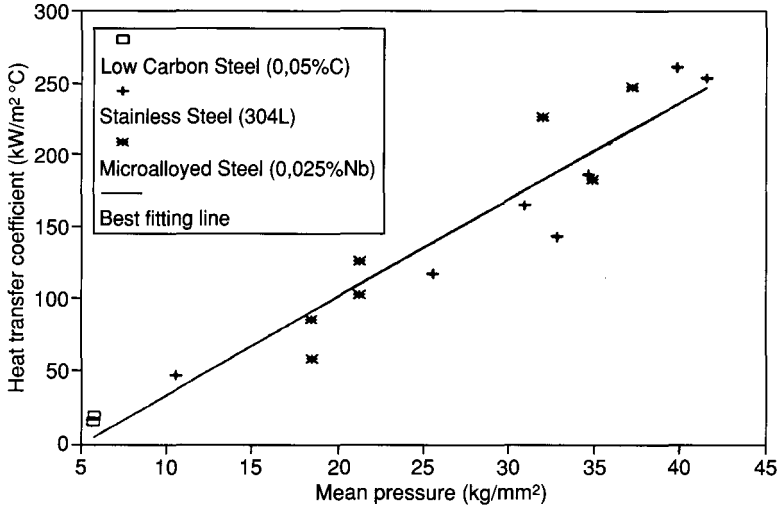

Figure 2—Relationship between the mean heat-transfer coefficient at the roll–steel interface and the mean pressure

Another factor that influences the thermal field is the presence of scale on the surface. The thermal conductivity of oxide scale is significantly lower than that of the parent metal, and consequently scale insulates the surface. To account for this, Chen[20] employed the equation of Ormerod *et al.*[21] to compute the thickness of the scale as a function of composition, temperature, and time. These equations were incorporated in a computer model that was developed to simulate the heat transfer during rough rolling, and the effect of scale formation on the thermal history of the slab was examined. The model ignores temperature variations in the transverse direction, but computes the temperature distribution in the two-dimensional plane through the centreline of the slab as a function of time. Thus, the temperature variation along the length of the slab was also computed[20]. In the model, it is assumed that the scale is perfectly adherent but is completely removed during descaling. During rolling, the scale is probably broken into a number of scale islands, but, for simplicity, it was assumed that the scale thickness decreases in proportion to the reduction of each pass, remains continuous over the surface of the slab, and grows in thickness during each interpass time. Based on the correlation between mean pressure and the mean heat-transfer coefficient for the roll bite, the heat-transfer coefficient for each pass was determined from the measured roll forces. The values for the seven passes are 50, 50, 50, 50, 52, 55, and 65 kW/m² respectively. Because the thickness of the scale layer formed on the slab surface during reheating varies[22] from 1,5 to 3,0 mm, an initial thickness of 2,0 mm was assumed in the model. The heat-conduction equation for both the steel and the oxide layer was solved with the aid of an implicit finite-difference technique.

Typical results illustrating the growth of the oxide scale during a seven-pass rolling operation are shown in Figure 3. Descaling was in effect after the second and sixth passes in this particular rolling operation. Notwithstanding the high temperatures, it is evident that only 100 μm of secondary scale grew during the roughing operation. However, because the thermal conductivity of the oxide scale is approximately one-tenth that of steel, its influence on the thermal field of the slab cannot be discounted.

niobium were rolled on a pilot and laboratory mill, and the thermal response was measured. Utilizing the model, heat-transfer coefficients for the roll- steel interface were computed, and the variables influencing this parameter were delineated.

A two-dimensional finite-element model was developed to predict the strain-rate, strain, and temperature distribution in the steel during deformation. To validate the model predictions, the computed strains were compared with measured strains, the latter having been determined in tests on a pilot mill.

Finally, a third model was developed to predict the microstructural evolution in carbon-manganese steels during finish rolling. The model incorporates empirical equations characterizing recrystallization and grain growth, and has been shown to be capable of predicting changes in austenite grain size during rolling in a finishing mill.

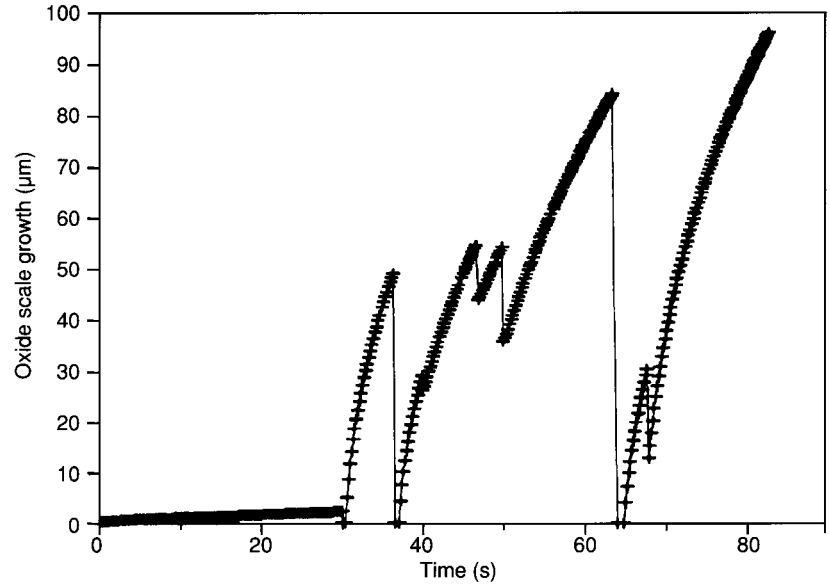

Figure 3—Variation of the thickness of the oxide scale on the surface of a slab during a seven-pass rough rolling operation

The influence of scale on the surface and subsurface temperatures halfway along the length of the slab in the seventh pass of a rough-rolling operation is illustrated in Figure 4. When there is a layer of oxide present, the surface temperature of the slab decreases rapidly at first and then rebounds in temperature owing to heat conduction from the interior. Furthermore, the oxide effectively insulates the steel and, as a result, the temperature of the scale–steel interface does not decrease very much in the roll bite. On the other hand, if there is no oxide, the surface temperature of the slab decreases by as much as 200°C in the roll bite.

The insulating effect of the scale also affects the final temperature distribution of the slab, as can be seen in Figure 5, where the thermal history of the surface and the centre of the slab, with and without oxidation, are compared for a seven-pass rolling operation. There is a difference of approximately 50°C in the predicted finishing temperature between the two cases. Hence, in the modelling of the thermal history of the rough-rolling operation, it is particularly important to include scale formation in the model. In finish rolling, since the total time is extremely short, the effects of oxide on the temperature of the transfer bar are minimal.

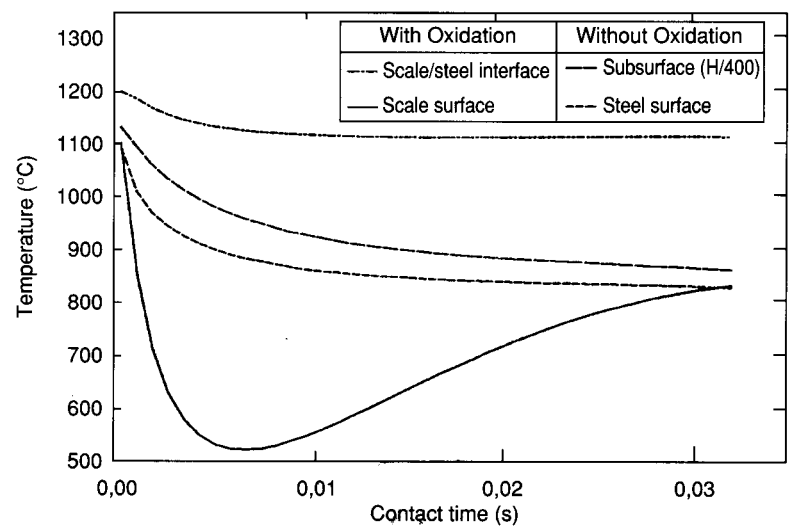

Figure 4—Temperature predictions for two locations in the slab during the seventh pass, with and without an oxide scale layer

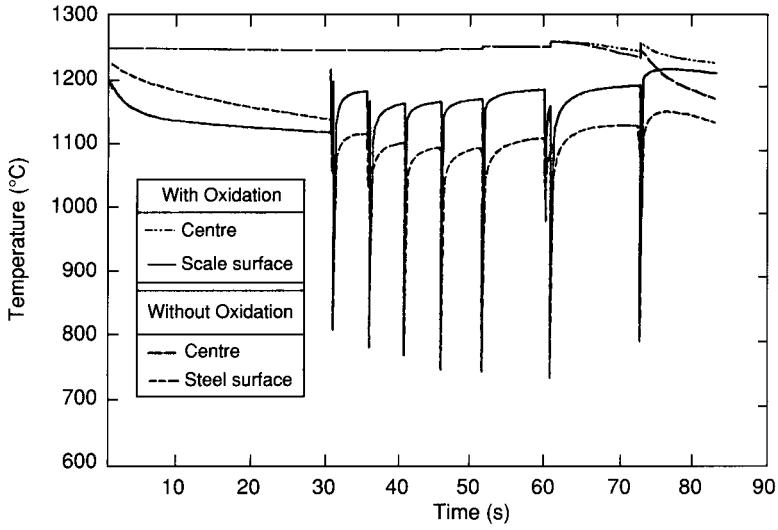

Figure 5—Comparison of predicted surface and centre temperature with and without an oxide scale layer for a seven-pass rough-rolling operation

Acknowledgements

The authors acknowledge the contributions of Dr C. Devadas (now with Comalco Research, Australia), Dr A. Kumar (from the Steel Authority of India Ltd), and Mr W.C. Chen (of UBC) to the research programme on the hot rolling of steel. The cooperation of Research and Development personnel at Stelco is appreciated. The authors are grateful for the financial support provided by the Natural Sciences and Engineering Research Council of Canada, by Stelco, and by Algoma.

References

1. SELLARS, C.M. *Material Sci. Tech.*, vol. 1.1985. p. 325.
2. SELLARS, C.M. *Int. Conf. on Physical Metallurgy of Thermomechanical Processing of Steels and Other Metals, THERMEC 88, Tokyo.* Tamura, I. (ed.). Tokyo, Iron and Steel Institute of Japan, 1988. p. 448.
3. SELLARS, C.M. *Proc. Int. Conf. on Hot Working and Forming Processes.* Sellars, C.M., and Davies, C.J. (eds.), London, The Metals Society of London, 1980. p. 3.
4. SELLARS, C.M., and WHITEMAN, J.A. *Met. Sci.*, 1979. p. 187.

Prediction of the thermomechanical behaviour during rolling

In recent years, the finite-element method has been employed to analyse the flat-rolling process because it permits a more accurate determination of the strain and strain-rate distribution in the roll bite. Widespread application of this tool to steel rolling has not occurred, but will be essential if microstructural changes are to be accurately predicted. Of the numerous techniques, the flow-formulation method is particularly suitable because of its capability of handling large deformations. This technique has been employed by several researchers to model deformation during hot rolling, with very limited attempts to validate the model[5, 23–26]. Kumar *et al.*[27] recently applied a two-dimensional formulation based on this method to finish rolling assuming plane strain, and demonstrated that the predicted roll forces depend critically on the equation employed to quantify the mechanical behaviour of steel at hot-rolling temperatures. The formulation proposed by Rao and Hawbolt[28] (given below) was employed in the model to compute the deformation resistance of the steel.

$$\dot{\varepsilon} = A\sinh(\alpha\sigma)^n \exp\left(-\frac{Q}{RT}\right),$$

where $\dot{\varepsilon}$ = strain rate, s^{-1}
σ = flow stress, kg/mm^2
α = empirical constant
A = constant
Q = activation energy, kJ/mol
R = gas constant, $kJ/mol^{-1}\ °C^{-1}$
T = temperature, °C
n = exponent.

Q, n, and $\ln A$ are related to strain ε through an expression of the form

$$Y = \frac{A_i}{\varepsilon^{B_i}} + C_i.$$

The basic variables in the flow-formulation approach are velocities and pressure, from which the strain-rate distribution in the deformation zone can be computed. The strain distribution is required in the use of these constitutive equations. Kumar *et al.*[27] determined the effective strain distribution in the roll bite by integrating the effective strain rate along successive elements in the deformation path. The flow stress at each point was recomputed and utilized in the finite-element model to give a new distribution of strain rate and strain in the roll-bite zone. The procedure was then repeated until convergence was obtained. Figures 6 and 7 show the effective strain rate and strain distribution in the transfer bar during the first pass of the finishing operation at the hot-strip mill of Stelco's Lake Erie Works. The corresponding temperature distribution is shown in Figure 8. The effective strain rate in the steel is highest at the surface, at the entry to and at the exit from the roll bite. The strain rate at these locations is nearly seven times the nominal strain rate, owing to the high redundant shear associated with constraining the metal to flow into and out of the roll gap. In addition, from Figure 6 it is evident that there is a dead zone beneath the rolls, a little over halfway along the arc of contact where the strain rate is extremely low. The unhomogeneous deformation that occurs during rolling results in non-uniform strain through the thickness, as illustrated in Figure 7. The effective strain is higher at the surface than at the centre owing to the effects of redundant shearing.

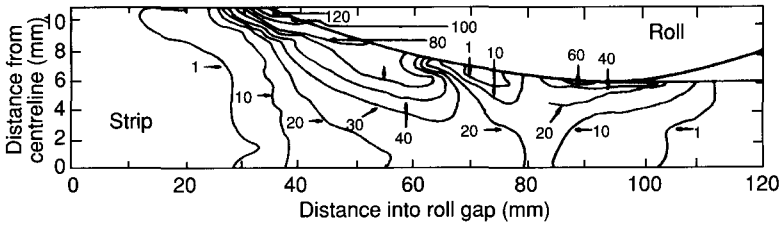

Figure 6—Computed effective strain-rate distribution in the roll bite for the first stand of a finishing mill

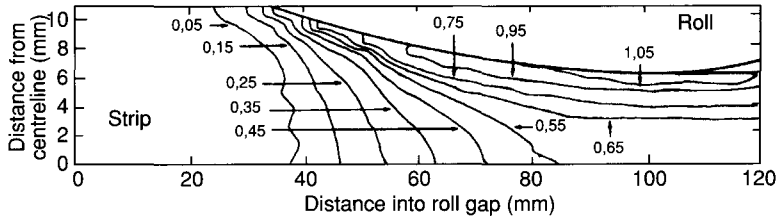

Figure 7—Computed effective strain distribution in the roll bite for the first stand of a finishing mill

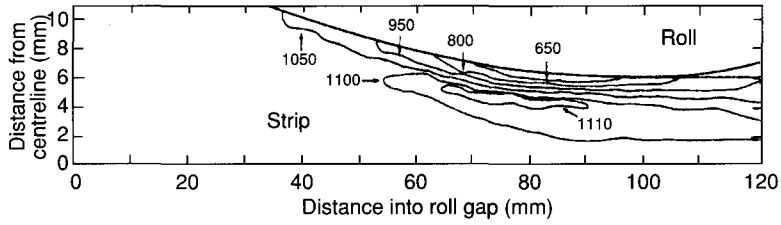

Figure 8—Predicted temperature in the roll bite for the first stand of a finishing mill

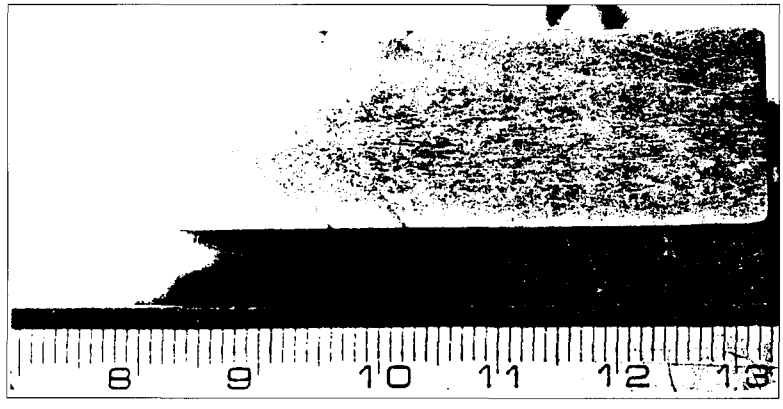

Figure 9—Photograph of a section through a sample containing a pin, after rolling, showing the deflection of the pin–sample interface

To validate the results of the finite-element model, several samples of AISI 304L stainless steel were instrumented with 5 mm diameter pins of the same material, the pin axis being perpendicular to the rolling direction[20]. After the samples had been rolled on the pilot mill at CANMET, they were sectioned and the strain distribution through the thickness[29] was computed from the curvature of the pin–sample interface. Figure 9 is a photograph of a sectioned sample after rolling, showing the deflection of the interface. The computed strain distribution is compared in Figure 10 with measured values determined from the interface shape for a test in which the sample was reduced 21,9 per cent. Good agreement was obtained between the measured and the predicted strain through the thickness except near the surface, where the model predictions were considerably higher than the measurements. This discrepancy may be due to the slight separation observed between the pin and the sample close to the surface (Figure 10). Notwithstanding this deficiency, both the finite-element model and the instrumented sample confirm that the strain is non-uniform through the thickness and that it increases towards the surface, as predicted by the model.

Microstructural evolution during hot rolling

The modelling of the microstructural evolution during hot rolling involved a selected set of equations to characterize the metallurgical phenomena in a thermomechanical model of the process. Existing correlations for recrystallization and grain growth for carbon–manganese steels, many of which are presented in Table II, were evaluated from comparisons of the predictions with experimental measurements made on 0,34 and 0,05 per cent carbon steels[14].

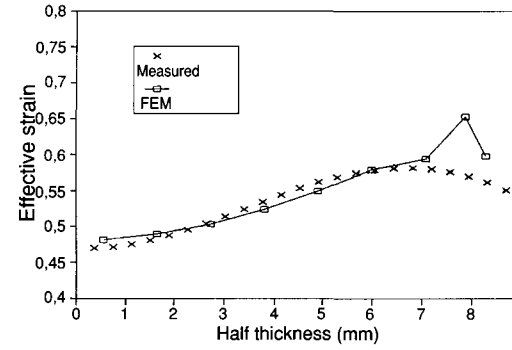

Figure 10—Comparison of the model-predicted through-thickness strains with measured strains determined from the curvature of the pin–sample interface

Table II

Summary of reported relationships for recrystallization and grain growth[14]

University of Sheffield Sellars and co-workers[1-5]	Nippon Steel Yada et al.[6-8]	Kawasaki Steel Saito et al.[9, 10]	IRSID Laboratories Perdix[11]
Dynamic recrystallization			
$\varepsilon_p = 4,9 \cdot 10^{-4} d_0^{1/2} Z^{0,15}$ $\varepsilon_c = \alpha\varepsilon_p$ $Z = \dot{\varepsilon} \exp \frac{Q}{RT}$ $Q = 312$ kJ/mol (metadynamic) $X = 1 - \exp\left(-0,693\left(\frac{t}{t_{0,5}}\right)\right)$	$\varepsilon_c = 4,76 \cdot 10^{-4} \exp\left(\frac{8000}{T}\right)$ $d_{dyn} = 22\,600 Z^{-0,27}$ $Z = \dot{\varepsilon} \exp \frac{Q}{RT}$ $Q = 267,1$ kJ/mol $X_{dyn} = 1 - \exp\left(-0,693\left(\frac{\varepsilon - \varepsilon_c}{\varepsilon_{0,5}}\right)^2\right)$ $\varepsilon_{0,5} = 1,144 \cdot 10^{-5} d_0^{0,28} \dot{\varepsilon}^{0,05} \exp\left(\frac{6420}{T}\right)$	$\varepsilon_c = 3,68 \cdot 10^{-4} Z^{0,19} d_0^{0,44}$ $d_{dyn} = 2,82 \cdot 10^4 Z^{-0,24}$ $Z = \dot{\varepsilon} \exp \frac{Q}{RT}$ $Q = 312$ kJ/mol	Not incorporated
Static recrystallization			
$X = 1 - \exp\left(-0,693\left(\frac{t}{t_{0,5}}\right)^2\right)$ $\varepsilon < 0,8\varepsilon_p$ $t_{0,5} = 2,5 \cdot 10^{-19} \varepsilon^{-4} d_0^2 \exp\left(\frac{Q_s}{RT}\right)$ $\varepsilon > 08\varepsilon_p$ $t_{0,5} = 1,06 \cdot 10^{-5} Z^{-0,6} \exp\left(\frac{Q_s}{RT}\right)$ $Q_s = 300$ kJ/mol $d_{rex} = 0,5 d_0^{0,67} \varepsilon^{-1}$ $(\varepsilon < \varepsilon^*)$ $d_{rex} = 1,8 \cdot 10^3 Z^{0,15}$ $(\varepsilon > \varepsilon^*)$ $\varepsilon^* = 0.57 d_0^{0,17} \varepsilon_p$	$X = 1 - \exp\left(-0,693\left(\frac{t}{t_{0,5}}\right)^2\right)$ $t_{0,5} = 2.2 \cdot$ $10^{-12} S_v^{-0,5} \dot{\varepsilon}^{-0,2} \varepsilon^{-2} \exp\left(\frac{30\,000}{T}\right)$ $d_{rex} = \frac{5}{S_v \varepsilon^{0,6}}$ $S_v = \frac{24}{\pi d_0}(0,491e^c = 0,155e^{-c}$ $+ 0,1433e^{-3c})$	$X = 1 - \exp\left(-0,693\left(\frac{t}{t_{0,5}}\right)^2\right)$ $t_{0,5} = 2,5 \cdot 10^{-19} \varepsilon^{-4} d_0^2 \exp\left(\frac{Q_s}{RT}\right)$ $Q_s = 300$ kJ/mol $d_{rex} = 0,5 d_0^{0,67} \varepsilon^{-1}$	$X = 1 - \exp\left(-0,693\left(\frac{t}{t_{0,5}}\right)^{n_r}\right)$ $t_{0,5} = 3,67 \cdot 10^{-14} \varepsilon^p \dot{\varepsilon}^{-0,28}$ $\cdot d_0^{0,14} \exp\left(\frac{Q_s}{RT}\right)$ $n_r = 272 d_0^{-0,155} \varepsilon^{-0,5}$ $\cdot \exp\left(\frac{-37,492}{RT}\right)$ $d_{rex} = 18,51 \ln\left(\frac{T}{973}\right)$ $\cdot d_0^{0,374} \varepsilon^m \dot{\varepsilon}^{-0,1}$ $u = -0,5 d_0^{0,267} \left(\frac{973}{T}\right)^{3,933}$ $p'' = -0,86 d_0^{0,24}$ $Q_s = 301$ kJ/mol
Grain growth			
$d^{10} = d_0^{10} + At \exp\left(\frac{-Q_{ss}}{RT}\right)$ $T > 1100°C$ $A = 3,87 \cdot 10^{32}$ $Q_{ss} = 400$ kJ/mol $T < 1100°C$ $A = 1,31 \cdot 10^{32}$ $Q_{ss} = 914$ kJ/mol	$d^2 = d_0^2 + At \exp\left(\frac{-Q_{ss}}{RT}\right)$ $A = 1,44 \cdot 10^{12}$ $\frac{Q_{ss}}{R} = 31\,100$	$d^{10} = d_0^{10} + At \exp\left(\frac{-Q_{ss}}{RT}\right)$ $T > 1100°C$ $A = 3,87 \cdot 10^{32}$ $Q_{ss} = 400$ kJ/mol $T < 1100°C$ $A = 1,31 \cdot 10^{32}$ $Q_{ss} = 914$ kJ/mol	$d = d_{rex}\left(1 + \alpha \ln \frac{t}{t_{rex}}\right)$ $\alpha = 0,195$ (C - Mn - Al steels) $\alpha = 0,098$ (Nb grades)

5. Beynon, J.H., Brown, P.R., Mizban, S.I., Ponter, A.R.S., and Sellars, C.M. *Proc. of NUMIFORM Conf., Gothenburg, Sweden.* Rotterdam (Holland), 1986. p. 213.

To determine the degree of static recrystallization during thermomechanical processing, single-hit Gleeble compression tests were conducted on a 0,34 per cent carbon steel at two temperatures (900°C and 850°C), at a strain rate of $1s^{-1}$. Following deformation, individual test samples were helium-quenched (30°C/s and 40°C/s) after delay times of 0,5, 2, 5, and 10 seconds. The helium quench enhanced the visibility of the prior austenite grain boundaries by encouraging the growth of pro-eutectoid ferrite on these boundaries during quenching.

6. YADA, H. *Proc. Int. Symp. Accelerated Cooling of Rolled Steel, Conf. of Metallurgists, CIM, Winnipeg, MB, Canada.* Ruddle, G.E., and Crawley, A.F., (eds.). Pergamon Press, Canada, 1987. p. 105.
7. SENUMA, T., and YADA, H. Annealing processes, recovery, recrystallization and grain growth. *Proc. 7th Riso Int. Symp. on Metallurgy and Materials Science.* Hansen. S.S., Juul Jensen, D., Lefjers, T., and Ralph, B. (eds.). Roshilde (Denmark), Riso National Laboratory, 1986. p. 547.
8. SUEHIRO, M., SATO, K., TSUKANO, Y., YADA, H., SENUMA, T., and MATSUMARA, Y. *Trans. ISIJ*, vol. 27. 1987. p. 439.
9. SAITO, Y., ENAMI, T., and TANAKA, T. *Ibid.*, vol. 25. 1985. p. 1146.

The metallographically observed recrystallization for the 0,34 per cent carbon steel at the two test temperatures (850°C and 900°C) for different delay times was compared with predictions based on equations proposed by Sellars[3] and IRSID[11], as shown in Table II. It is clear that the IRSID equation yielded better agreement with the metallographic observations. Double-hit compression tests were conducted on the Gleeble at UBC and on the camplastometer at CANMET in a determination of the recrystallization kinetics from fractional softening. The Avrami pre-exponential and time exponent constants were determined from the data for each grade by use of the appropriate $t_{-0,5}$ relationships listed in Table II. The results were employed to calculate the recrystallization curves shown in Figures 11 and 12, based on both the Sellars and the IRSID analyses. It can be seen that the IRSID equations gave good agreement with the measurements. Thus, in the model developed at UBC, the IRSID equations were employed.

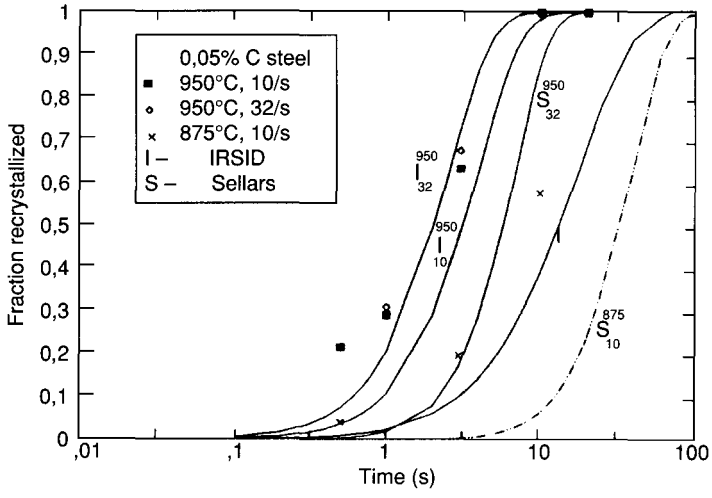

Figure 11—Comparison of the measured fractional softening and the predicted recrystallization kinetics for the 0,05 per cent carbon steel

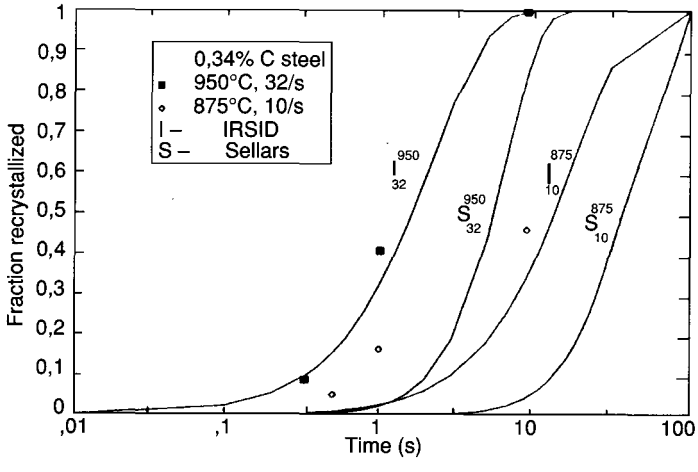

Figure 12—Comparison of the measured fractional softening and the predicted recrystallization kinetics for the 0,34 per cent carbon steel

From Table II, it is evident that dynamic recrystallization is treated less rigorously than static recrystallization in many models. In the current model, the instantaneous strain in the roll bite was compared with the critical strain calculated from the expression given by Sellars[3] to show whether dynamic recrystallization was likely to initiate. If it is likely, then metadynamic recrystallization kinetics are employed in place of static recrystallization kinetics in the interstand region.

The literature does not appear to give data on the grain growth of high-temperature austenite immediately following recrystallization in the short time interval of 0 to 2 seconds corresponding to interstand times on a hot-strip mill. The empirical correlations proposed by various researchers are generally based on grain growths corresponding to longer times. In the study described here, the following equation was used in the calculation of grain growth:

$$d^{7,5} = d_{rex}^{7,5} + 4,2 \times 10^{27} t \exp\left(\frac{-400}{RT}\right)$$

d = instantaneous grain diameter, μm
d_{rex} = statically recrystallized grain size, μm
t = time, s.

The constants in this equation were obtained from regression analyses on data obtained by Hawbolt and his co-workers[30] for a eutectoid plain-carbon steel isothermally annealed at temperatures of 800°C to 1100°C for growth times extending to 600 seconds.

Selected equations characterizing static-metadynamic recrystallization and grain growth were employed in the modelling of microstructure evolution in the hot-strip mill at Stelco's Lake Erie Works. The temperature distribution in the roll bite at each stand was computed with the heat-transfer model[12]. The principle of additivity was extremely useful in the modelling of non-isothermal conditions because it allows isothermal kinetic data for recrystallization and grain growth to be employed for the determination of structural changes occurring during continuous cooling and heating[31-33], as occurs in rolling. As a first approximation, strain and strain-rate variations through the thickness were ignored, and were computed from the pass reduction. The strain was assumed to be uniform for each vertical slice and the strain rate to be constant in the roll bite. These simplifications will be revised in the next generation of models. An important difference between the current work and many of the earlier studies is that the temperature distribution in the steel, both within and outside the roll bite, was characterized accurately.

10. SAITO, Y., SAEKI, M., NISHIDA, M., ITO, Y., TANAKA, T., and TAKIZAWA, S. *Proc. Int. Conf. on Steel Rolling,* Toky,. Iron and Steel Institute of Japan, 1980. p. 1309.
11. CH. PERDRIX. Characteristic of plastic deformation of metals during hot working. *Report* CECA no. 7210 EA/311, Saint Germain-en-Laye (France), Institute de Recherches de la Siderurgie Francaise (IRSID), 1987.
12. DEVADAS, C., SAMARASEKERA, I.V., and HAWBOLT, E.B. *Metall. Trans.,* vol. 22A. 1991. p. 307.
13. DEVADAS, C., BARAGAR, D., RUDDLE, G., SAMARASEKERA, I.V., and HAWBOLT, E.B. *Ibid.,* p. 321.
14. DEVADAS, C., SAMARASEKERA, I.V., and HAWBOLT, E.B. *Ibid.,* p. 335.
15. CAMPBELL, P.J., HODGSON, P.D., LEE, M., and GIBB, R.K. *Int. Conf. on Physical Metallurgy of Thermomechanical Processing of Steels and Other Metals, THERMEC 88, Tokyo.* Tamura, I. (ed.). Tokyo, Iron and Steel Institute of Japan, 1988. p. 761.
16. GIBBS, R.K., and HODGSON, P.D. *Morris E. Fine Symposium.* Liaw, P.K., Weertman, J.R., Marcus, H.L., and Santner, J.S. (eds.). The Minerals, Metals and Materials Society, 1991. p. 73.
17. LAASRAOUI, A., and JONAS, J.J. *ISIJ International,* vol. 31, no. 1. 1991. p. 95.
18. CHEN, W.C., SAMARASEKERA, I.V., and HAWBOLT, E.B. *Mech. Working and Steel Processing Conference Proceedings.* Iron and Steel Society of AIME, 1991.
19. SAMARASEKERA, I.V. *Proc. Int. Symposium on the Mathematical Modelling of Hot Rolling of Steel, 29th Annual Conference of Metallurgists, CIM, Hamilton, Ontario, Canada.* Yue, S., Hawbolt, E.B., Too, J.J.M., and Stachowiak, R. (eds.). 1990. p. 145.
20. CHEN, W.C. Thermomechanical phenomena during rough rolling. M. A. Sc. thesis, University of British Columbia, 1991.

To validate the microstructural model, a series of tests was conducted on the pilot mill at CANMET in which determinations were made of the changes to austenite grain size as a result of one to four passes of rolling, each pass simulating an individual stand of the hot-strip mill at Stelco's Lake Erie Works prior to the addition of a fifth stand. The details of the rolling schedules on the industrial mill are given in Table III and the mill simulations in Table IV. The first test in Table IV is a simulation of the first stand, the second a simulation of stands I and II, the third a simulation of stands I to III, and the fourth a simulation of all four stands.

A comparison of Tables III and IV shows that the rolling temperature and the degree of reduction experienced in successive stands of the Lake Erie mill were effectively reproduced in the CANMET simulation tests. However, it is impossible to simulate, on CANMET's reversing mill, the short interstand times and high strain rates realized in the production mill for stands III and IV. Prior to rolling, each sample was reheated to the desired temperature in the programmable, atmosphere-controlled reheating facility. The rolled samples were quenched in an icebath within a period of 5 seconds after each test. The quenched samples were etched so that the prior austenite grain size could be determined. The microstructural model was employed to simulate the tests, and the model-predicted grain size were compared with measurements on samples quenched after one or more deformation passes. The results are illustrated in Figure 13, which shows the centreline and surface temperatures computed by the heat-transfer model. The starting grain size in the simulation tests was 180 µm, corresponding to the prior austenite grain size measured on the transfer bar samples. The measured grain sizes after passes I, II, and III, were observed to be 67 µm, 34 µm, and 25 µm respectively, which compares well with the model predictions. After the fourth pass, an increase in the measured grain size was observed contrary to predictions. The reason for this increase in grain size is not known, but could be due to errors in the measurements of the rolling temperature.

Table III

A typical rolling schedule at Stelco's Lake Erie Works mill prior to the addition of the fifth stand

Pass number	Reduction %	Mean strain rate s^{-1}	Centre temperature °C	Interstand time s
I	43	17,6	1077	3,04
II	41	38,0	1060	1,8
III	25	49,9	1020	1,2
IV	17	57,1	970	-

Table IV

Simulation tests conducted on the CANMET pilot mill for the assessment of microstructural change in a 0,34 per cent carbon steel

Number of passes	Reheating temp. °C	Reduction %	Strain rate s^{-1}	Centre temp. °C	Interstand time s	Quench time s
1	1100	43	17,5	1060	-	5
2	1100	43	17,5	1067	10	5
		41	33,3	1040		
3	1100	43	17,4	1060	11	5
		41	33,1	1030	9.5	
		25	30,4	986		
4	1120	43	17,4	1070	11	6
		41	33,2	1057	8	
		25	30,3	1009	10	
		17	27,4	923		

21. ORMEROD IV, R.C., BECKER, H.A., GRANDMAISON, E.W., POLLARD, A., RUBINI, P., and SOBIESIAK, A. *Proc. Int. Symp. on Steel Reheat Furnace Technology, 29th Annual Conference of Metallurgists, CIM, Hamilton, Ontario, Canada.* Mucciardi, F. (ed.). 1990. p. 227.
22. HOLLANDER, F. *Proc. Conf. Mathematical Models for Metallurgical Process Development.* London, The Iron and Steel Institute, 1970. p. 46.
23. ZIENKIEWICZ, O.C., JAIN, P.C., and ONATE, E. *Int. J. Solids and Structures,* vol. 14. 1978. p. 15.
24. DAWSON, P.R. *Application of Numerical Methods in Forming Processes.* San Francisco, Winter Meeting of the American Soc. Mech. Eng., 1974. p. 55.
25. ZIENKIEWICZ, O.C., ONATE, E., and HEINRICH, J.C. *Int. J. for Numerical Methods in Engineering,* vol. 17. p. 1497.
26. DAWSON, P.R. *Int. J. of Solid Structures,* vol. 23, no. 7. 1987. p. 947.
27. KUMAR, A., SAMARASEKERA, I.V., and HAWBOLT, E.B. Roll bite deformation during the hot rolling of steel strip. *J. of Materials Processing,* 1991.
28. RAO, K.P., and HAWBOLT, E.B. Development of simple constitutive relationships for use in high temperature deformation models. *Trans Am. Soc. Mech. Eng.,* Engineering Materials Tech., 1991.
29. SAKAI, T., SAITO, Y., HIRANO, K., and KATO, K. *Trans. ISIJ,* vol. 28. 1988. p. 1028.
30. HAWBOLT, E.B., BRIMACOMBE, J.K., and CHAU, B. The University of British Columbia, Vancouver, B.C. Canada, unpublished research, 1989.
31. MAGEE, K.E. M. A. Sc. thesis, University of British Columbia, Vancouver, B.C. Canada, 1986.
32. HAWBOLT, E.B., CHAU, B., and BRIMACOMBE, J.K. *Metall. Trans. A.,* vol. 16A. 1985. p. 565.
33. KUBAN, M.B., JAYARAMAN, R., HAWBOLT, E.B., and BRIMACOMBE, J.K. *Metall. Trans. A,* vol. 17A. 1986. p. 1493.

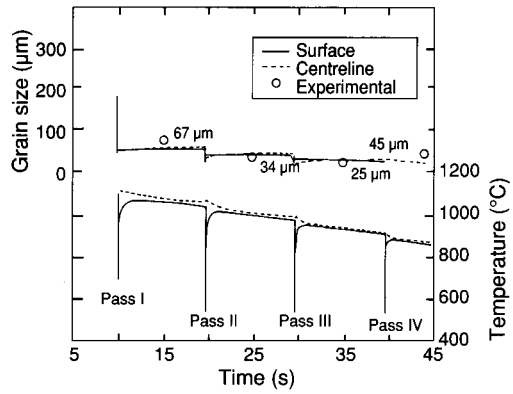

Figure 13—Comparison of the predictions of the microstructural model with the experimentally measured grain size obtained from the pilot-mill simulation at CANMET on a 0,34 per cent carbon steel

In an examination of the capability of the model to simulate an industrial rolling schedule, it was used to compute the changes in austenite grain size during the rolling of a 0,05 per cent carbon steel on the mill at Stelco's Lake Erie Works prior to the addition of the fifth stand. The changes in grain size between the centre and the surface are shown in Figure 14, along with the fraction recrystallized. The percentage reductions at each successive pass were 34, 36, 36, and 21,5 respectively. As expected, the model predicted complete recrystallization between passes and, in this particular instance, there was little difference in grain size between the centre and the surface. The entry temperature for the same grade was varied in steps of 50°C in the model to show the effect of this variable on the final grain size. A 200°C decrease in entry temperature, from 1214°C to 1014°C, resulted in a 20 μm reduction in final grain size, as illustrated in Figure 15. The increased grain size at the higher rolling temperatures can be seen to be largely due to grain growth at these higher temperatures.

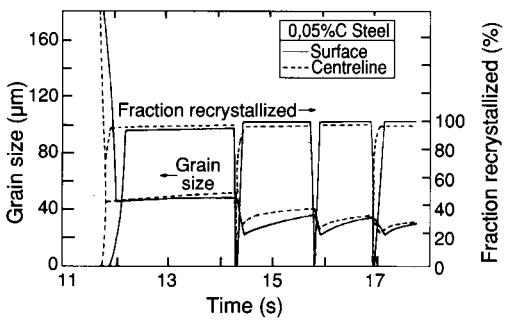

Figure 14—Predicted evolution of the austenite grain size and the fraction recrystallized during the rolling of a 0,05 per cent carbon steel in the hot-strip mill at Stelco's Lake Erie Works

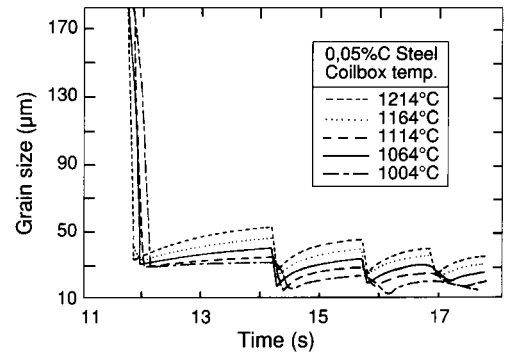

Figure 15—Predicted effect of the rolling temperature on the computed grain size

Summary and conclusions

The modelling of microstructural evolution that has been conducted at UBC in the past few years includes the following.

- Measurements of the thermal response of instrumented samples during rolling on the laboratory mill at the university and on a pilot mill at CANMET were used to give heat-transfer coefficients at the roll–steel interface for a variety of conditions. It was shown that a strong correlation exists between the mean pressure and the mean heat-transfer coefficient in the roll bite, irrespective of the type of material or the rolling conditions. This correlation was used in the determination of heat-transfer coefficients at the roll–steel interface during industrial rolling.
- A mathematical model of heat transfer was developed to predict the temperature distribution along the length of a slab during rough rolling. The model also simulates the growth of oxide scale on the slab surface. It was shown that, during rough rolling, the scale formed insulates the surface of the slab, reducing the heat transfer to the work rolls. The difference between the model-predicted finishing temperature, with and without oxide scale, for a seven-pass rough-rolling operation was approximately 50°C.
- A two-dimensional finite-element model based on the flow-formulation method was used in studies of the deformation during hot rolling. The model predictions were validated by comparison with measurements on rolled samples. It was shown that the strain is unhomogeneous through the thickness and is at a maximum at the surface.
- The changes to austenite grain size during the finish rolling of carbon–manganese steels was predicted successfully. ◆